

compared to Ni(DPPE)Cl₂. However, Pd(DPPE)Cl₂ (70:30, HT:HH) was not nearly as effective as Ni(DPPE)Cl₂. The smaller ionic radius of Ni²⁺ vs Pd²⁺ along with the higher steric demands for DPPE indicate that the degree of stereoregularity is controlled by steric congestion of the reductive elimination step. This is further supported by the fact that **3** is apparently isomerized into **2** (by a series of transmetalation–reductive elimination followed by oxidative addition) faster than it is polymerized.

The ¹H and ¹³C NMR spectra of PHT provide sensitive probes of the substitution pattern in the polymer backbone. In a mixture of the four possible triad regioisomers (Figure 1a structures), all of the vinyl carbon atoms (16 peaks are theoretically possible) and all of the vinyl protons (4 total) can be resolved.^{1a,b,7} This is clearly demonstrated in the ¹H and ¹³C NMR spectra of **4** (Figures 1a and 2a). The observed spectra are consistent with a totally random (1:1:1:1, HT-HT:HT-HH:TT-HT:TT-HH linkages based on NMR integration) mixture of the four triad structures depicted.

In contrast, only one sharp band for the vinyl proton, which denotes the HT-HT structure, and four sharp bands for the vinyl carbon atoms (one band for each carbon), which also denotes the HT-HT structure, are observed in the ¹H and ¹³C NMR spectra of **5** (Figures 1b and 2b). The resolution and signal:noise ratio characterize **5** as pure HT-PHT (98.5 ± 1.5%). The two doublet peaks (7.15, 6.93 ppm) and one singlet peak at 6.91 ppm (Figure 1a) are assigned as the terminal ring protons Ha, Hb, and Hc of PHT.⁸

The molecular weights were determined by GPC (relative to polystyrene standard). Random PHT has $M_w = 2.44 \times 10^4$ and $M_n = 5.65 \times 10^3$, corresponding to a polydispersity index of 4.32. HT-PHT does not completely dissolve in THF at the same concentration; the soluble part has $M_w = 1.50 \times 10^4$. UV–vis data shows that HT-PHT has the longest wavelength of maximum absorption either in solution (CHCl₃, 456 nm) or in the solid state (film, 560 and 610 nm) when compared with the values of other PHT.^{1a,b,2b,9} This indicates that HT-PHT has the greatest effective conjugation length in the polymer chain, apparently due to complete head-to-tail regularity.¹⁰ Random PHT has maximum absorption with the relatively shorter wavelengths of 427 (CHCl₃) and 438 nm (film). The physical properties for the two polymers are quite different.¹¹

Neither regioregular HT-PHT, such as **5**, nor equally random PHT, such as **4**, has previously been reported.^{1a,b,2c} We expect the regioregular HT-PHT to have a large improvement not only in electrical conductivity but also in magnetic, nonlinear optical properties and other physical properties, and we are currently pursuing such characterizations. Likewise we are examining aspects of this polymerization which may explain the difference in control of regiochemistry observed in Ni and Pd catalysis.

Acknowledgment. This work was supported by grants from the National Institutes of Health (GM35153). We thank Prof. R. T. Hembre for his helpful discussions and Prof. C. H. James Wang and Mr. Xuanqi Zhang for help with the MW determination. We thank Drs. R. A. O'Brien, H. Xiong, L. Zhu and B. T. Dawson as well as Douglas Stack and Walter Klein.

Supplementary Material Available: Synthetic procedures for **4** and **5**, ¹H and ¹³C NMR spectra, and tables of IR, GC, and elemental analysis data (9 pages). Ordering information is given on any current masthead page.

(7) (a) Sato, M.-s.; Morri, H. *Polym. Commun.* **1991**, *32* (2), 42. (b) Sato, M.-s.; Morri, H. *Macromolecules* **1992**, *24*, 1196.

(8) Mao, H.; Holdcroft, S. *Macromolecules* **1992**, *25*, 554.

(9) Rughooputh, S. D. V.; Hotta, S.; Heeger, A. J.; Wudl, F. *J. Polym. Sci., Part B: Polym. Phys.* **1987**, *25*, 1071–1078.

(10) Roux, C.; Leclerc, M. *Macromolecules* **1992**, *25*, 2141–2144.

(11) The solubility of random PHT in chloroform is at least 3 times greater than that of regioregular HT-PHT apparently due to the reduced crystallinity of the polymer chain. More interestingly, a film of the regular HT-PHT is gold-yellow in color, with a metallic luster and a strong fluorescence; the random polymer only forms a red-brown transparent film.

Generation and Reactivity of the First Mononuclear Early Metal Phosphinidene Complex, Cp*₂Zr=P(C₆H₂Me₃-2,4,6)

Zhaomin Hou and Douglas W. Stephan*

Department of Chemistry and Biochemistry
University of Windsor, Windsor, Ontario, Canada N9B 3P4

Received July 30, 1992

The wide-ranging applications of metal carbenes (M=C) in organometallic chemistry¹ have spawned interest in transition metal complexes containing metal–heteroatom double bonds. While many metal–oxo and –sulfido systems are generally robust, recent work has shown that early metal systems containing metal–imido (M=NR),^{2–4} –oxo (M=O),^{5–8} and –sulfido (M=S)⁸ have a rich chemistry. Development of related early metal phosphinidene (M=PR) chemistry faces several obstacles. Firstly, synthetic routes to known phosphinidene complexes typically involve either use of metal complex anions or thermal degradation of coordinated phosphinidene precursors.⁹ Neither of these methods is amenable to early metals. A second problem is the propensity of phosphinidene moieties to bridge two or more metal centers. Thus, while V¹⁰ and Zr¹¹ phosphinidene-bridged complexes have been characterized, related mononuclear systems are unknown.¹² Herein, we describe the preparation of the primary phosphide complex Cp*₂Zr(PH(C₆H₂Me₃))₂ (**1**). This species is a synthon for a transient mononuclear Zr=PR moiety which reacts intramolecularly with sp³ C–H bonds, with P–H bonds or MeCN affording phosphametalloacycles.

The reaction of Cp*₂ZrCl₂ with 2 equiv of LiPH(C₆H₂Me₃) in benzene at 25 °C gave the wine-red diphosphido species **1**^{13,14} in 90% isolated yield. In the solid state the pseudotetrahedral zirconium center resides on a crystallographically imposed 2-fold

(1) *Metal-Ligand Multiple Bonds*; Nugent, W. A., Mayer, J. M., Eds.; John Wiley and Sons: New York, 1988.

(2) Walsh, P. J.; Hollander, F. J.; Bergman, R. G. *J. Am. Chem. Soc.* **1988**, *110*, 8729.

(3) Walsh, P. J.; Carney, M. J.; Bergman, R. G. *J. Am. Chem. Soc.* **1991**, *113*, 6343.

(4) Walsh, P. J.; Hollander, F. J.; Bergman, R. G. *J. Organomet. Chem.* **1992**, *428*, 13.

(5) Parkin, G.; Bercaw, J. E. *J. Am. Chem. Soc.* **1989**, *111*, 391.

(6) Carney, M. J.; Walsh, P. J.; Hollander, F. J.; Bergman, R. G. *J. Am. Chem. Soc.* **1989**, *111*, 8751.

(7) Whinnery, L. L.; Hening, L. M.; Bercaw, J. E. *J. Am. Chem. Soc.* **1991**, *113*, 7575.

(8) Carney, M. J.; Walsh, P. J.; Bergman, R. G. *J. Am. Chem. Soc.* **1990**, *112*, 6426.

(9) (a) Huttner, G. *Pure Appl. Chem.* **1986**, *58*, 585. (b) Mathey, F. *Angew. Chem., Int. Ed. Engl.* **1987**, *26*, 275.

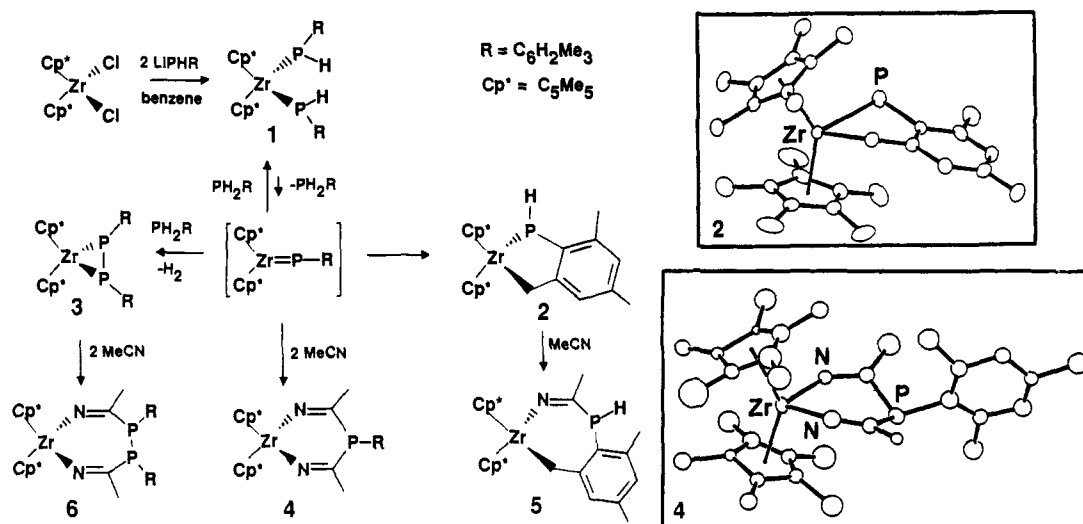
(10) Arif, A. M.; Cowley, A. H.; Pakulski, M.; Norman, N. C.; Orpen, A. G. *Organometallics* **1987**, *6*, 189.

(11) Ho, J.; Stephan, D. W. *Organometallics* **1991**, *10*, 3001.

(12) Only two transition metal complexes containing terminal phosphinidene moieties have been structurally characterized: (a) Cowley, A. H.; Pellerin, B. *J. Am. Chem. Soc.* **1990**, *112*, 6734. (b) Hitchcock, P. B.; Lappert, M. F.; Leung, W. P. *J. Chem. Soc., Chem. Commun.* **1987**, 1282. (c) The ³¹P NMR chemical shifts of the “bent” terminal phosphinidene complexes are as follows: Cp₂Mo=P(C₆H₂(*t*-Bu)₃), 799.5 ppm; Cp₂W=P(C₆H₂(*t*-Bu)₃), 661.1 ppm. (d) DME may stabilize the adduct Cp*₂Zr(μ-P(C₆H₂Me₃))₂(μ-Cl)Li(DME).

(13) In all cases, C₆H₂Me₃ refers to the 2,4,6-trimethylphenyl substituent. NMR data (all recorded in C₆D₆ at 25 °C, δ (ppm) relative to TMS and 85% H₃PO₄ for ¹H and ³¹P data, respectively): **1**: ³¹P{¹H} NMR δ 39.0; ¹H NMR δ 6.91 (s, 4 H), 4.43 (d of m, 2 H, |J_{P-H}| = 268 Hz, |J_{P-H}| = 50 Hz), 2.73 (br s, 6 H), 2.60 (br s, 6 H), 2.26 (s, 6 H), 1.72 (s, 30 H). **2**: ³¹P{¹H} NMR δ -42.6; ¹H NMR δ 6.86 (s, 1 H), 6.73 (s, 1 H), 3.54 (d, 1 H, |J_{P-H}| = 180 Hz), 2.75 (s, 3 H), 2.26 (s, 3 H), 1.72 (s, 30 H), 1.25 (s, 2 H). **3**: ³¹P{¹H} NMR δ 134.9; ¹H NMR δ 6.93 (s, 2 H), 6.73 (s, 2 H), 3.33 (s, 6 H), 2.29 (s, 6 H), 1.78 (s, 30 H), 1.24 (s, 6 H). **4**: ³¹P{¹H} NMR δ 0.2; ¹H NMR δ 6.89 (s, 2 H), 2.15 (s, 3 H), 1.99 (d, 3 H, |J_{P-H}| = 4.5 Hz), 1.89 (s, 30 H), 1.87 (br s, 6 H). **5**: ³¹P{¹H} NMR δ -71.9; ¹H NMR δ 6.88 (s, 1 H), 6.58 (s, 1 H), 5.36 (d, 1 H, |J_{P-H}| = 225 Hz), 2.29 (s, 3 H), 2.19 (s, 3 H), 2.08 (d, 3 H, |J_{P-H}| = 3.6 Hz), 1.76 (s, 15 H), 1.54 (s, 15 H), 1.26 (s, 2 H). **6**: ³¹P{¹H} NMR δ -30.1; ¹H NMR δ 6.80 (s, 4 H), 6.49 (s, 4 H), 3.03 (s, 6 H), 2.40 (s, 6 H), 2.07 (t, 6 H, |J_{P-H}| = 1.5 Hz), 1.99 (s, 30 H), 1.94 (s, 6 H). Satisfactory combustion analyses have been obtained for **1–6**.

Scheme 1



axis of symmetry with a Zr–P bond length of 2.63 (2) Å, which is typical of pyramidal phosphinides on Zr(IV).

Compound 1 is a synthon for the highly reactive phosphinidene intermediate Cp*₂Zr=P(C₆H₂Me₃) as judged by its subsequent trapped products. Monitoring of a benzene solution of 1 by ³¹P NMR showed the slow loss of the resonance attributable to 1 and the growth of signals attributable to two new Zr complexes, free primary phosphine PH₂(C₆H₂Me₃), and traces of (PH(C₆H₂Me₃))₂. The new Zr complexes were isolated by fractional crystallization. After 2 days, red-brown crystals of 2 were deposited. The NMR spectra¹³ and crystallographic data¹³ confirmed 2 as the phosphametallocycle Cp*₂Zr(CH₂C₆H₂Me₃PH). Upon further standing for several days, a second new Zr derivative, Cp*₂Zr(PC₆H₂Me₃)₂ (3), was obtained.¹³

Bergman et al.² have described the generation of Cp₂Zr=NR from Cp₂Zr(NHR)₂. In our case, a similar equilibrium between 1 and the highly reactive phosphinidene intermediate accounts for the conversion of 1 to 2 and 3. Intramolecular C–H bond activation of an *o*-methyl group in the transient phosphinidene accounts for the formation of 2. Formation of 3 requires addition of the P–H bond of the primary phosphine to the Zr=P double bond with the opposite regiochemistry to that which permits re-formation of 1. This yields a P–P bond, and subsequent elimination of H₂ drives the irreversible formation of 3. Compound 2 is stable in solution, even in the presence of excess phosphine (PH₂(C₆H₂Me₃)) and is thus not involved in the formation of 3. Interception of the transient phosphinidene was achieved via the reaction of a solution of 1 with MeCN in benzene at 25 °C. The products include free primary phosphine PRH₂ as well as the yellow-orange six-membered metalocycle Cp*₂Zr(NCMe)₂P(C₆H₂Me₃) (4).^{13,14} The geometry at the phosphorus atom in 4 is pseudopyramidal. Mechanistically, this reaction may be viewed as a 2 + 2 cycloaddition of MeCN to the phosphinidene with subsequent insertion of a second equivalent of acetonitrile into the Zr–P bond. Attempts to observe the initial cycloaddition product led only to the observation of 1, 4, and free phosphine. Although attempts to isolate the phosphinidene intermediate have been unsuccessful to date, direct spectroscopic evidence for a phosphinidene species is derived from the reaction of LiPH-

(C₆H₂Me₃) and Cp*₂ZrCl₂ in DME at 25 °C. In addition to 1, a ³¹P NMR resonance at 537 ppm with no P–H coupling is seen. This downfield resonance is attributed to the unstable bent phosphinidene intermediate.^{12c,d} Addition of MeCN to this DME solution led to the disappearance of both the resonance at 537 and that from 1 and the appearance of the signal from 4. Attempts to trap this species employing dative donors such as PMe₃ were unsuccessful, affording instead mixtures of 2 and 3.

It was also found that reactions of 2 and 3 with MeCN give quantitatively the seven-membered metalocycles Cp*₂Zr(CH₂C₆H₂Me₃PH(C(Me)N)) (5) and Cp*₂Zr(NC(Me)P(C₆H₂Me₃))₂ (6), respectively.¹³

The chemistry described herein illustrates that generation of a reactive phosphinidene intermediate offers a route to a variety of new phosphametallocycles and thus a point of entry for metal-mediated organophosphorus chemistry.

Acknowledgment. The financial support from NSERC of Canada is gratefully acknowledged.

Supplementary Material Available: Tables of crystallographic data, thermal and hydrogen atom parameters, and selected bond distances and angles for 1, 2, 4, and 6 (33 pages); listing of observed and calculated structure factors for 1, 2, 4, and 6 (40 pages). Ordering information is given on any current masthead page.

Is the Structure of Selenoformamide Similar to Those of Formamide and Thioformamide?

Jerzy Leszczyński,* Józef S. Kwiatkowski,*[†] and Danuta Leszczyńska

Department of Chemistry
Jackson State University
Jackson, Mississippi 39217

Received April 15, 1992

Formamide and its thio and seleno analogs can formally exist in two tautomeric forms, 1 and 2 (Chart I). However, it is experimentally well documented that the amide form 1 of both formamide (F) and thioformamide (SF) is a dominating species in the vapor phase, an inert environment, and a polar medium.¹

(14) Crystal data, 1: C₃₈H₅₄P₂Zr, *Pbcn*, *a* = 10.941 (4) Å, *b* = 15.719 (6) Å, *c* = 21.047 (9) Å. 2: C₂₉H₄₁PZr, *P2₁/n*, *a* = 11.724 (8) Å, *b* = 15.613 (6) Å, *c* = 14.791 (3) Å, β = 102.81 (3)°. 4: C₃₃H₄₇N₂PZr, *Pbcn*, *a* = 23.328 (6) Å, *b* = 18.777 (5) Å, *c* = 14.583 (6) Å. 6: C₄₂H₅₈N₂P₂Zr, *Cc*, *a* = 16.722 (33) Å, *b* = 14.003 (3) Å, *c* = 17.652 (9) Å, β = 104.04 (9)°. Mo K α radiation, λ = 0.71069 Å, and a Rigaku AFC6-S diffractometer were employed to collect the data (4.5° < 2 θ < 50°). The solutions were obtained and refined employing the TEXSAN software package from MSC. Refinement (data *I* > 3 σ (*I*), variables *R*, *R_w*), 1: 309, 55, 0.0962, 0.0967. 2: 2740, 280, 0.0480, 0.0554. 4: 916, 111, 0.0857, 0.0850. 6: 1570, 212, 0.0411, 0.0482.

[†] Permanent address: Instytut Fizyki, Uniwersytet M. Kopernika, 87-100 Toruń, Poland.